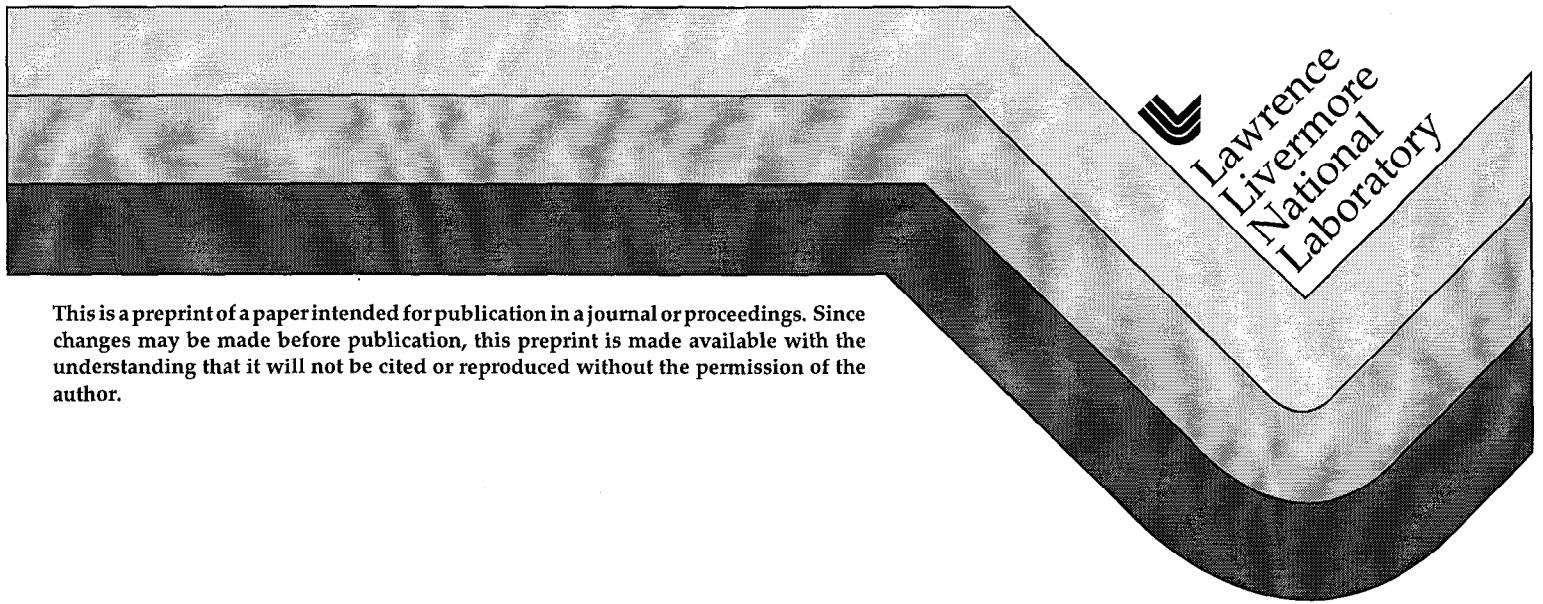# Improving m_b:M_s Discrimination Using Phase Matched Filters Derived from Regional Group Velocity Tomography

M.E. Pasyanos
W.R. Walter
S.R. Ford
S.E. Hazler

DISCLAIMER

IMPROVING m_b:M_S DISCRIMINATION USING PHASE MATCHED FILTERS DERIVED FROM REGIONAL GROUP VELOCITY TOMOGRAPHY

Michael E. Pasyanos, William R. Walter, and Sean R. Ford
Lawrence Livermore National Laboratory
Geophysics and Global Security Division
Livermore, CA 94551, USA

Shannon E. Hazler
Department of Geology and Geophysics
University of Colorado
Boulder, CO 80309, USA

ABSTRACT

This study reports on the ongoing investigation of surface wave group velocity dispersion across the Middle East and North Africa. Using broadband data gathered from various sources, we have measured group velocity using a multiple narrow-band filter method. To date, we have examined over 13,500 seismograms and made quality measurements for about 6500 Rayleigh and 3500 Love wave paths. A conjugate gradient method is used to perform the group velocity tomography at several periods. There is excellent agreement between short period structure and large known sedimentary features. Longer period structure is sensitive to crustal thickness, particularly the contrast between continental and oceanic regions and thicker crusts found beneath orogenic zones. We also find slow upper mantle velocities along rift systems. Correlation between the inversion results and known major tectonic features gives us confidence in our surface wave group velocities.

Accurate group velocity maps can be used to construct phase matched filters. The filters can improve weak surface waves by compressing the dispersed signal. We are particularly interested in using the filters to calculate regionally determined M_s measurements, which we hope can be used to extend the threshold of m_b:M_s discriminants to lower magnitude levels. A preliminary analysis of surface wave data processed using phase matched filters indicates a significant improvement in increasing the signal-to-noise ratio and improving magnitude estimates. Where signal-to-noise is very poor, phase matched filtering can still be useful in lowering the upper bound on M_s measurements. We propose a series of tests in order to analyze the utility of phase matched filters. Goals of the study include determining at what distance and magnitude ranges we can expect to see improvement using the filters and the overall effect of the filters on discrimination capability. We also propose to look at seismic velocity models of the Middle East and North Africa region in order to test the discrimination performance achieved using the various models.

Key Words: surface waves, group velocity, discrimination, tomography, Middle East, North Africa

OBJECTIVE

The purpose of this research is 1) to improve surface wave group velocity maps and lithospheric shear wave velocity models for the Middle East and North Africa, and 2) use the group velocity results in phase-matched filters in order to lower M_s thresholds and improve m_b:M_s discrimination. M_s is an important discriminant measure and phase-matched filters could help identify smaller magnitude events. Improved shear velocity should improve event location capabilities throughout the region. Both improved identification and location capabilities are important to monitoring the Comprehensive Nuclear-Test-Ban Treaty. This work is on-going and to date we have concentrated on measuring Rayleigh and Love wave group velocities for paths in the region and tomographically inverting the measurements. We are currently starting to focus more on the discrimination aspect of this research.

RESEARCH ACCOMPLISHED

Group Velocity Measurements and Inversion

Using broadband data gathered from various sources, we have measured group velocity using a multiple narrow-band filter method. To date, we have examined over 13,500 seismograms and made quality measurements for about 6500 Rayleigh and 3500 Love wave paths. Path maps for a number of periods are shown in Figure 1. In general, we have the most paths for periods between 40 and 60 seconds, with the number of paths dropping off at both shorter and longer periods. We also have about twice as many Rayleigh waves as Love waves at a particular period. In Figure 1, for example, we have 3000 paths for 20 second Rayleigh waves, 5000 paths for 50 second Rayleigh waves, 1700 paths for 20 second Love waves, and 2100 paths for 50 second Love waves.

A conjugate gradient method is used to perform the group velocity tomography at several periods. We perform the group velocity inversions for both Rayleigh and Love waves between 10 and 100 seconds at 5 second intervals at periods shorter than 30 seconds and at 10 second intervals beyond. A more complete analysis of the inversion method, uncertainty, resolution and damping is given in Pasyanos, et al [1999]. Results for several periods between 15 and 50 seconds are shown for Rayleigh and Love waves in Figures 2 and 3, respectively.

Results

There is excellent agreement between short period structure and known large-scale sedimentary features. Rayleigh wave maps between 10 and 15 seconds and Love wave maps between 10 and 20 seconds highlight shallow sedimentary basins (i.e. whole Mediterranean Basin, northern Indian Ocean). Meanwhile, Rayleigh wave maps between 20 and 30 seconds and Love wave maps between 25 and 40 seconds emphasize only the deepest basins (i.e. Eastern Mediterranean, Caspian Basin, Persian Gulf, Mesopotamian Foredeep). In some cases, we can see a great likeness between Rayleigh and Love wave maps. For example, at 20 second Rayleigh waves and 30 second Love waves, which are both sensitive to deep sedimentary features, the maps are quite similar.

Longer period inversions (40 - 50 second Rayleigh waves and 50 - 60 second Love waves) are sensitive to crustal thickness, particularly the contrast between continental and oceanic regions and thicker crusts found beneath orogenic zones. At the longest periods in our study (> 60 second Rayleigh waves and > 70 second Love waves), our inversions are increasingly sensitive to the mantle, such as the slow upper mantle velocities along rift systems. Correlation between the inversion results and known major tectonic features gives us confidence in our surface wave group velocities, as does the correspondence between Rayleigh and Love wave maps. Additionally, our group velocity maps are very similar to those performed in Eurasia (Ritzwoller and Levshin, 1998) in regions where the two studies overlap.

The group velocity maps can be used to invert for shear wave structure in the Middle East and North Africa. In addition, the group velocity tomography can be combined with other data, such as P_n tomography and phase velocity tomography (see Hazler, et al, this volume) to reduce non-uniqueness in the model and develop the most complete P-wave and S-wave structure of the region. This is especially important in aseismic regions, where surface waves are one of the only methods of studying the area. The resulting three-dimensional velocity model would be useful for improving location of seismic events, as well as for characterizing the propagation of regional phases (i.e. L_g) which are useful for discrimination.

Phase Matched Filters

Phase-matched filters can improve weak surface wave signals by compressing the dispersed signals (Herrin and Goforth, 1977). The compressed signals can be cleaned to exclude noise sources such as microseismic noise, multipathing, body waves, higher order surface waves, and coda. With this methodology it is possible to extract surface wave signals from noisy measurements, calculate regionally determined M_s measurements, and lower the threshold on surface wave magnitude measurements. Much research has already been performed on surface wave analysis using phase-matched filters. For example, Stevens and McLaughlin, [1997] focused on using a 5 degree by 5 degree model to improve magnitude estimates globally. In our study the emphasis is on using our high-resolution surface wave tomography in the filters in order to make regional surface wave magnitude estimates in our region. These, in turn, can be combined with m_b to form one of the best known discriminants of earthquakes and explosions. Using phase matched filters derived from our high-resolution tomography, we hope to more accurately get at smaller events in our area and lower the m_b:M_s discriminant to even lower magnitude levels.

We can construct group velocity correction surfaces for a station, wavetype (i.e. LR, LQ), and period. A background velocity model for the correction surface is produced by integrating slownesses for the appropriate period and wavetype from the station to all points on the grid. We then employ the kriging methodology to create the correction surfaces (Schultz, et al 1998). The surface is made by kriging residuals formed from comparisons between the measurements made at that station and the tomographically-derived background velocity model. The kriged residuals are then added back to the velocity model back to produce the final correction surface. For a given station and source location, we can simply look up the group velocities to use in the phase-matched filter. An example of a correction surface for 50 second Rayleigh waves at station ABKT (Alibek, Turkmenistan) is shown in Figure 4.

Filter Performance

A preliminary analysis of surface wave data processed using phase-matched filters indicates a significant improvement in increasing the signal-to-noise ratio and making more robust magnitude estimates. Where signal-to-noise is very poor, phase matched filtering can still be useful in lowering the upper bound on M_s measurements. We intend to test discrimination performance by examining the m_b:M_s discriminant for the Indian and Pakistani nuclear tests at nearby stations. Figure 5a shows single-station M_s measurements made at station AAK (Ala Archa, Kyrgyzstan) using a phase-matched filter. In this case, the phase-matched filters were derived from only the surface wave tomography, without the addition of kriging. The M_s measurements are compared to m_b estimates from the PDE. The trend between the two sets of magnitudes are shown by the dotted line. In addition, we plot the theoretical relation between the two magnitudes predicted by equilibrating the Gutenburg and Richter energy relationships for m_b and M_S. There is a variation of about one magnitude unit around the trend that is probably due to a combination of factors, but is likely most attributable to variations in surface wave radiation caused by the source mechanism.

Figure 5b shows the difference between the M_s measurements made using the phase-matched filter and the measurements made without it. In general, use of the phase-matched filter results in lowering the measured M_s, with the greatest improvement seen in the m_b 4.5-5.5 range for this $\Delta > 20°$ dataset. There is a significant portion of the data (events with excellent signal-to-noise) in which the use of the filter has no effect on M_s. We propose to conduct a series of tests in order to analyze the utility of phase-matched filters. Goals of the study include determining at what distance and magnitude ranges we can expect to see improvement using the filters and the overall effect of the filters on discrimination capability.

The phase-matched filters used in Figure 5 were derived using group velocities from our surface wave tomography. If the phase-matched filters were derived from another model, we would get different results. We propose to look at seismic velocity models of the Middle East and North Africa region in order to test the discrimination performance achieved using the various models. For example, in general how sensitive are our results to the base velocity model. How significant are any improvements between one-dimensional and two-dimensional models or between different two-dimensional models? Figure 6 shows one way of trying to assess model performance.

Figure 6a plots the surface wave magnitude that was determined for events both with and without phase-matched filters derived from the global model PREM (Dziewonski and Anderson, 1981), a model which we would not expect to have group velocities that are appropriate for the Middle East and North Africa. Even for the largest events, we note difference between the surface wave magnitudes calculated with and without the phase-matched

filters. In this case, the reason for the difference is that the inappropriate model is unable to predict the correct group velocity and a significant portion of the surface wave energy is coming in outside of the window. Since we are unable to recover the magnitude for the largest events, we have no confidence in the filter performance for the smaller events.

Figure 6b shows a similar magnitude plot determined with and without a phase-matched filter derived from the surface wave tomography. For the largest events, there is basically no difference in the M_s value determined using the filters indicating that, since the events had such good signal-to-noise ratio, the filters had little or no effect on the waveform. More importantly, it means that along all of these paths the envelope of group velocities predicted from the tomography was able to successfully predict the arrival time of the surface wave energy. For smaller magnitude events, starting around M 4.5, we can see that the magnitudes that were determined using the filter generally had smaller magnitudes. Unlike the previous case, where we were testing an inappropriate model, we can conclude that the lower magnitude levels are presumably due to a reduction in the noise that was contaminating the surface wave signal.

CONCLUSIONS AND RECOMMENDATIONS

We have made group velocity measurements of thousands of paths across the Middle East and North Africa. By tomographically inverting our measurements, we find that the Love and Rayleigh group velocities correlate well with tectonic structures, such as sedimentary basins, variations in crustal thickness, and upper mantle features. Over the whole period range examined, we find significant lateral variations of group velocities that diverge significantly from global models. As such, it is obviously inappropriate to use globally derived group velocity models as the basis for the phase-matched filters. We have found that the use of tomographically-derived background models produce suitable correction surfaces for the filters. The addition of kriging on top of these background models will further improve the correction surfaces. Having established an appropriate model to use as a basis for the phase-matched filters, we can now test the performance of the filters over a range of distances and magnitudes, ultimately assessing the overall improvement of our discrimination capability. High-resolution tomography models in the region can allow us to look at smaller magnitude events at shorter regional distances.

REFERENCES

Dziewonski, A. and D. Anderson (1981), Preliminary Reference Earth Model, *Phys. Earth Planet. Inter.*, 25, 297-356.

Herrin, E. and T. Goforth (1977), Phase-matched Filters: Applications to the Study of Rayleigh Waves, *Bull. Seism. Soc. Amer.*, 67, 1259-1275.

Pasyanos, M.E., W.R. Walter, S.E. Hazler (1999), A surface wave dispersion study of the Middle East and North Africa for Monitoring the Comprehensive Nuclear-Test-Ban Treaty, *submitted to Pure and Applied Geophysics*.

Ritzwoller, M.H., and A.L. Levshin (1998), Eurasian surface wave tomography: group velocities, *J. Geophys. Res.*, 103, 4839-4878.

Schultz, C., S. Myers, J. Hipp, and C. Young (1998), Nonstationary Bayesian kriging: a predictive technique to generate corrections for detection, location, and discrimination, *Bull. Seism. Soc. Amer.*, 88, 1275-1288.

Stevens, J.L. and K.L. McLaughlin (1997), Improved methods for regionalized surface wave analysis, Maxwell Technologies Technical Report to Phillips Laboratory, PL-TR-97-2135.
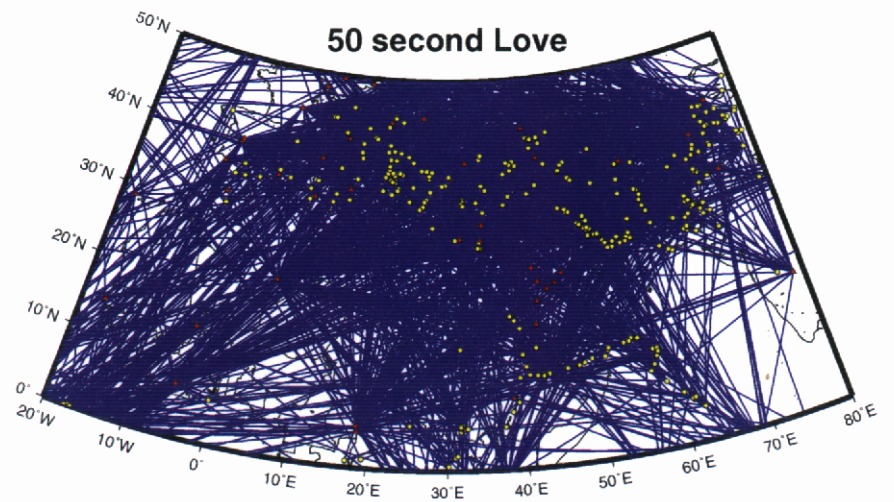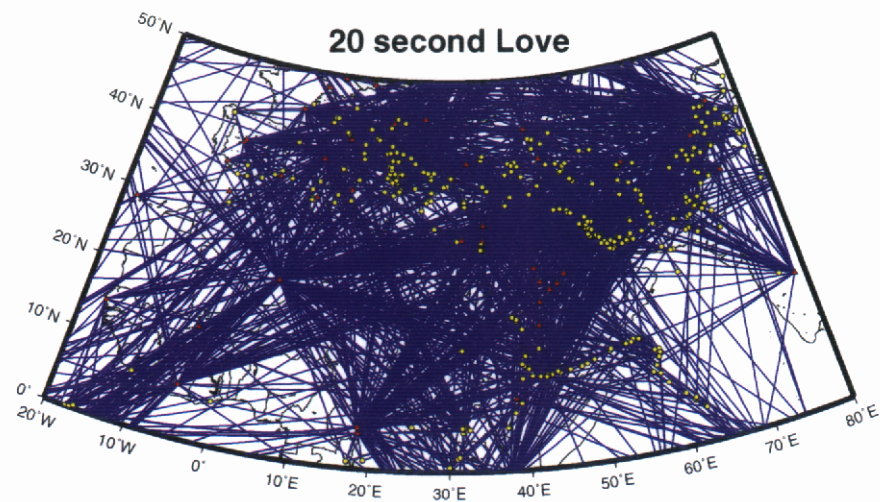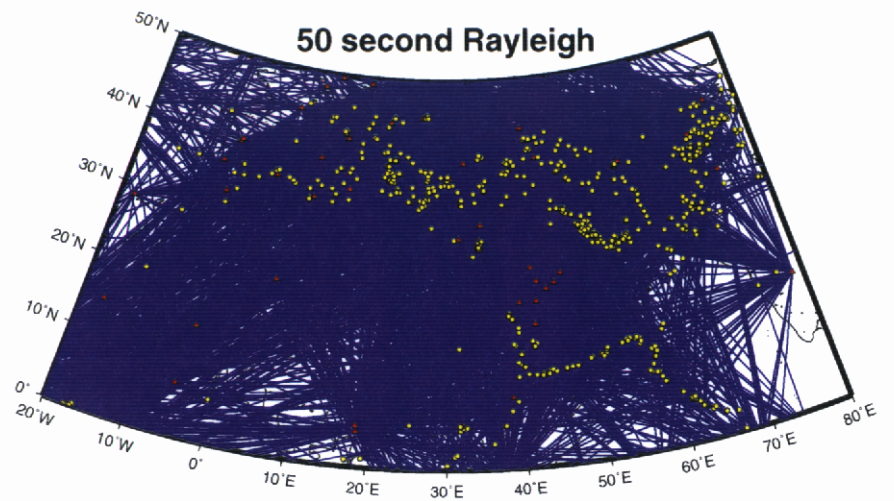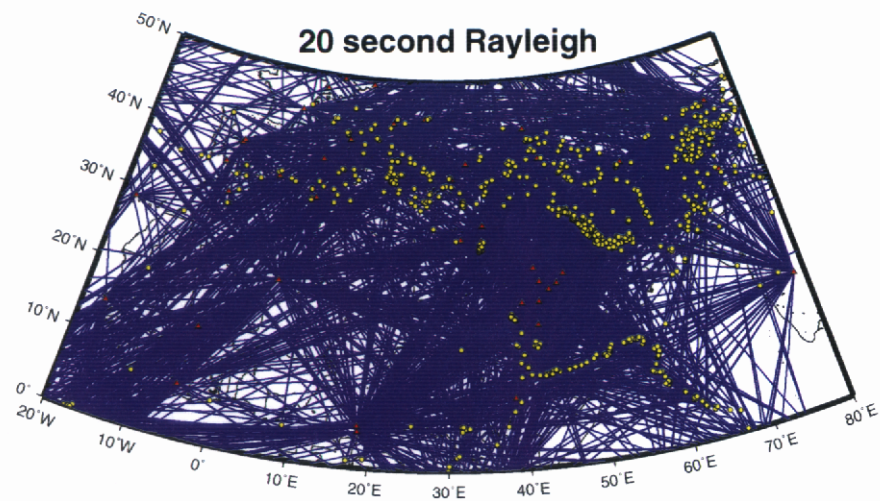
Figure 1 - Surface wave path maps for group velocities recorded for 20 sec Rayleigh waves, 50 sec Rayleigh waves, 20 sec Love waves, and 50 sec Love waves. Circles show earthquake locations, triangles show station locations.
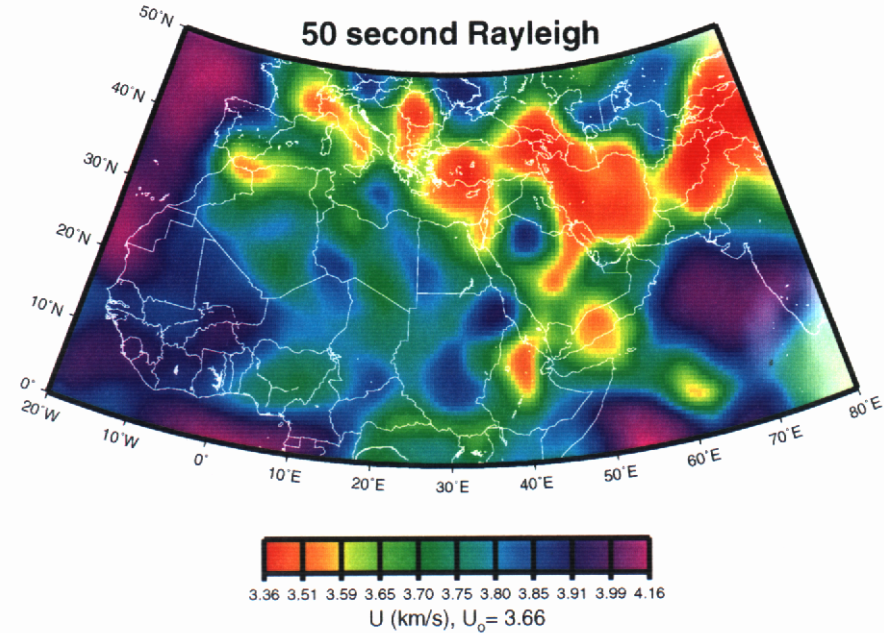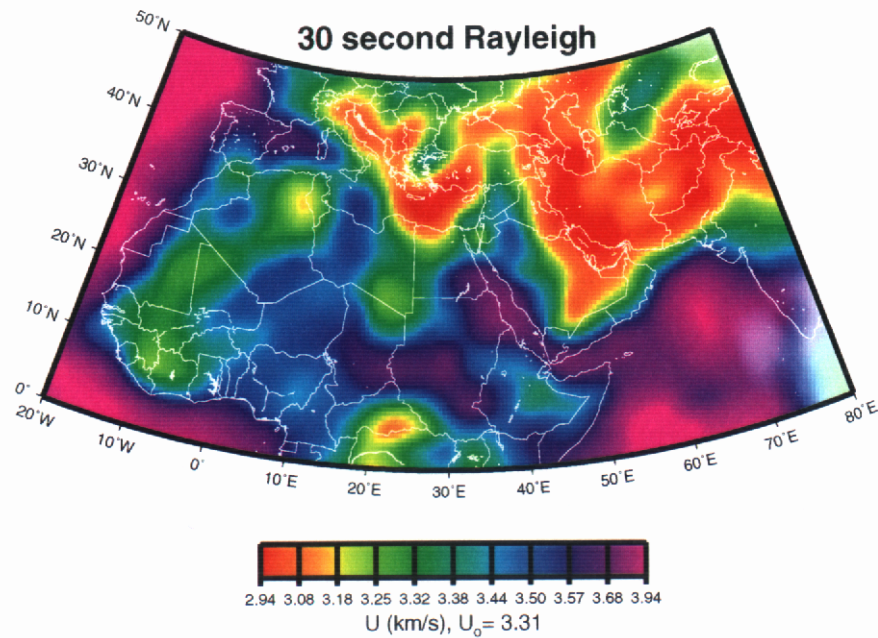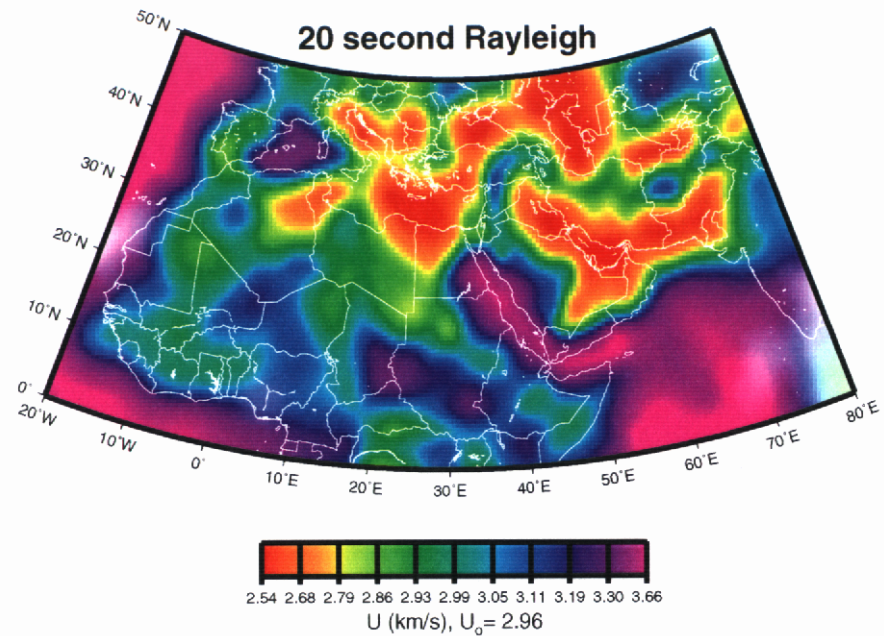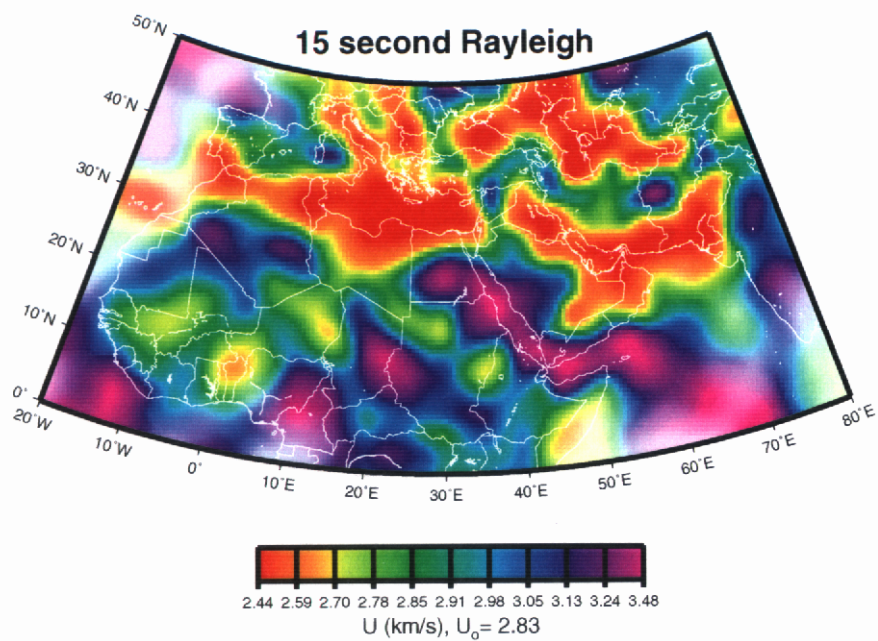
15 second Rayleigh

2.44 2.59 2.70 2.78 2.85 2.91 2.98 3.05 3.13 3.24 3.48

U (km/s), U_0 = 2.83

20 second Rayleigh

2.54 2.68 2.79 2.86 2.93 2.99 3.05 3.11 3.19 3.30 3.66

U (km/s), U_0 = 2.96

30 second Rayleigh

2.94 3.08 3.18 3.25 3.32 3.38 3.44 3.50 3.57 3.68 3.94

U (km/s), U_0 = 3.31

50 second Rayleigh

3.36 3.51 3.59 3.65 3.70 3.75 3.80 3.85 3.91 3.99 4.16

U (km/s), U_0 = 3.66

Figure 2 - Group velocity tomography for 15, 20, 30, and 50 sec Rayleigh waves. Velocities are indicated by the accompanying scale bars.

15 second Love
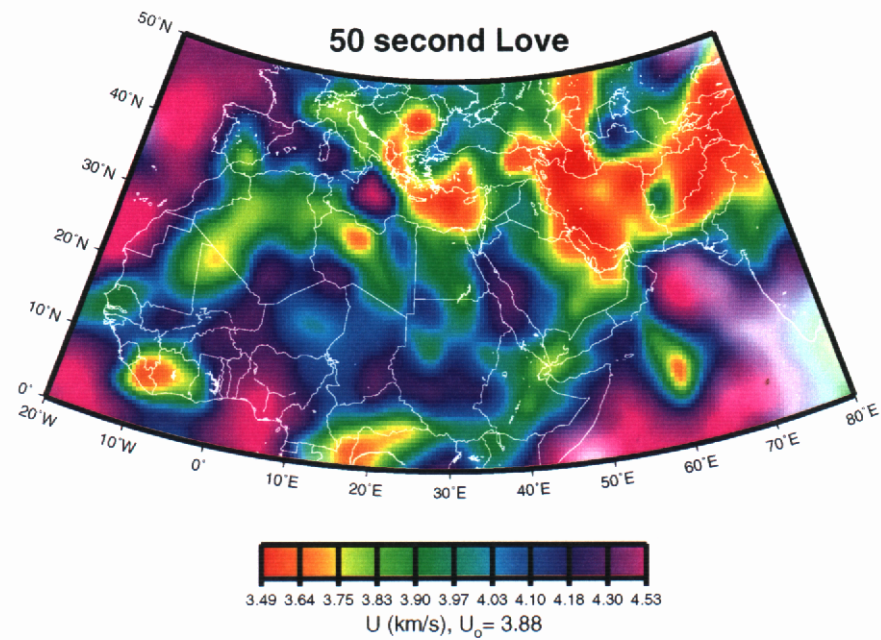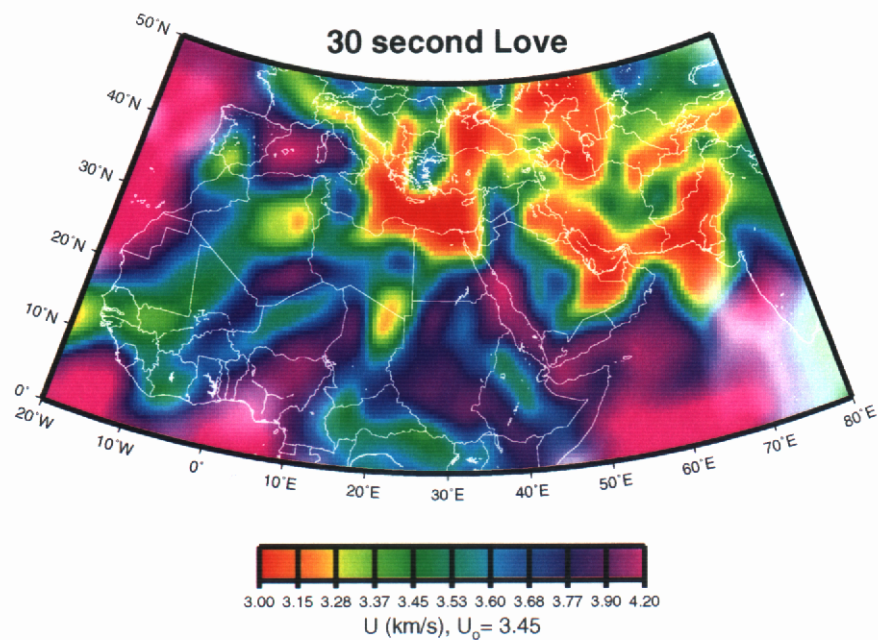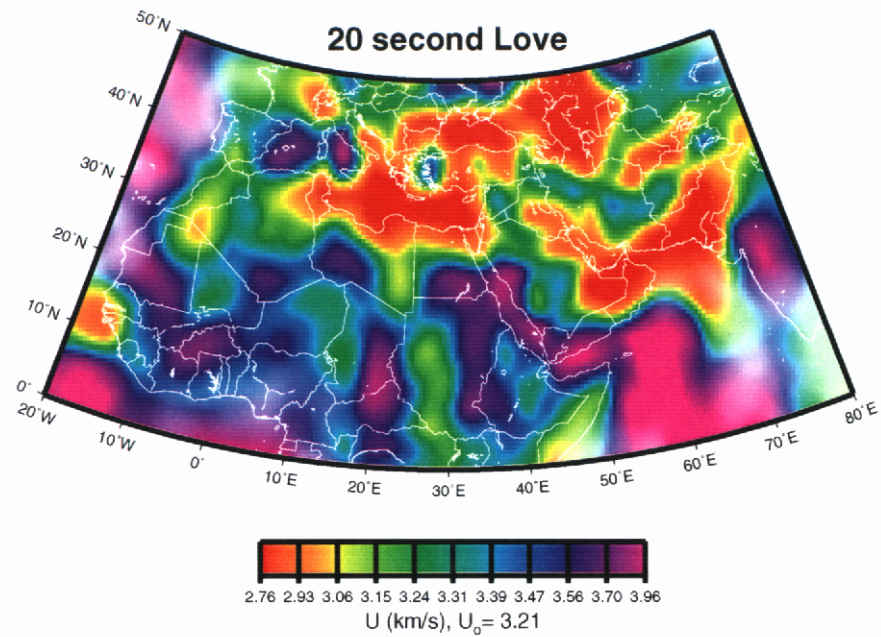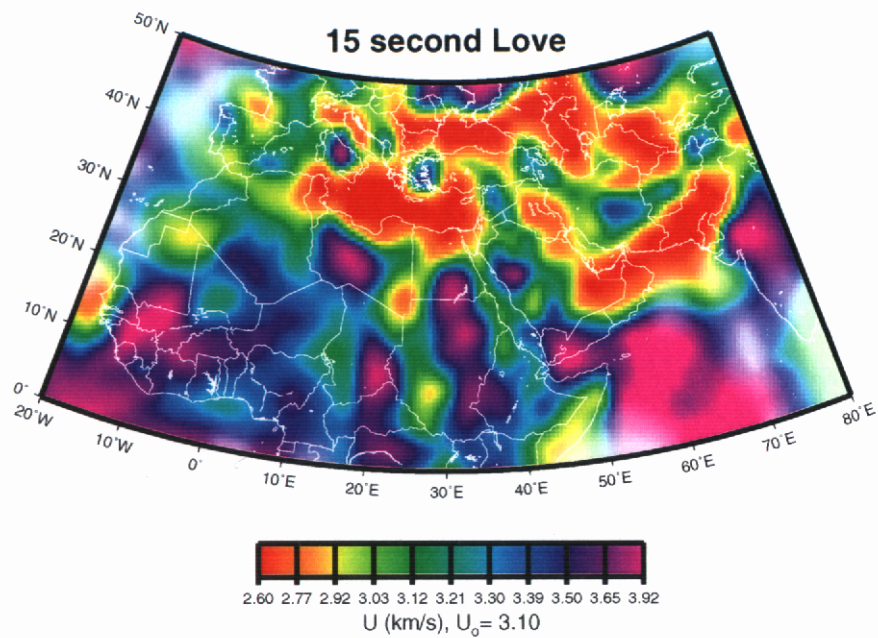
2.60 2.77 2.92 3.03 3.12 3.21 3.30 3.39 3.50 3.65 3.92
U (km/s), U_o = 3.10

20 second Love

2.76 2.93 3.06 3.15 3.24 3.31 3.39 3.47 3.56 3.70 3.96
U (km/s), U_o = 3.21

30 second Love

3.00 3.15 3.28 3.37 3.45 3.53 3.60 3.68 3.77 3.90 4.20
U (km/s), U_o = 3.45

50 second Love

3.49 3.64 3.75 3.83 3.90 3.97 4.03 4.10 4.18 4.30 4.53
U (km/s), U_o = 3.88

Figure 3 - Group velocity tomography for 15, 20, 30, and 50 sec Love waves. Velocities are indicated by the accompanying scale bars.
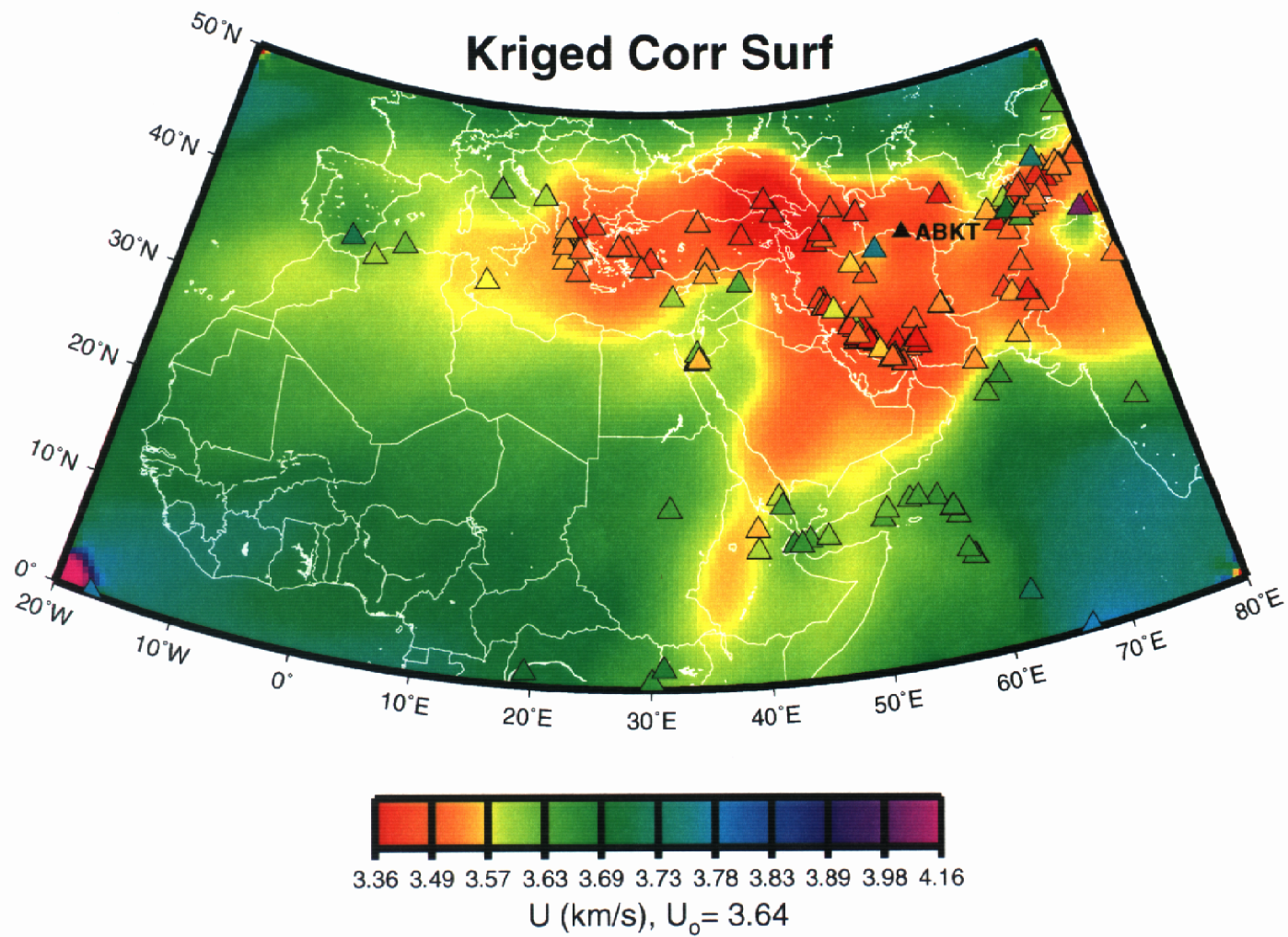
Figure 4 - Correction surface for 50 second Rayleigh waves at station ABKT produced by kriging group velocity observations made at that station (triangles) on a background model derived from the tomography.

AAK (pmf)

M_s

$Ms=0.9789mb-0.8434$

GR
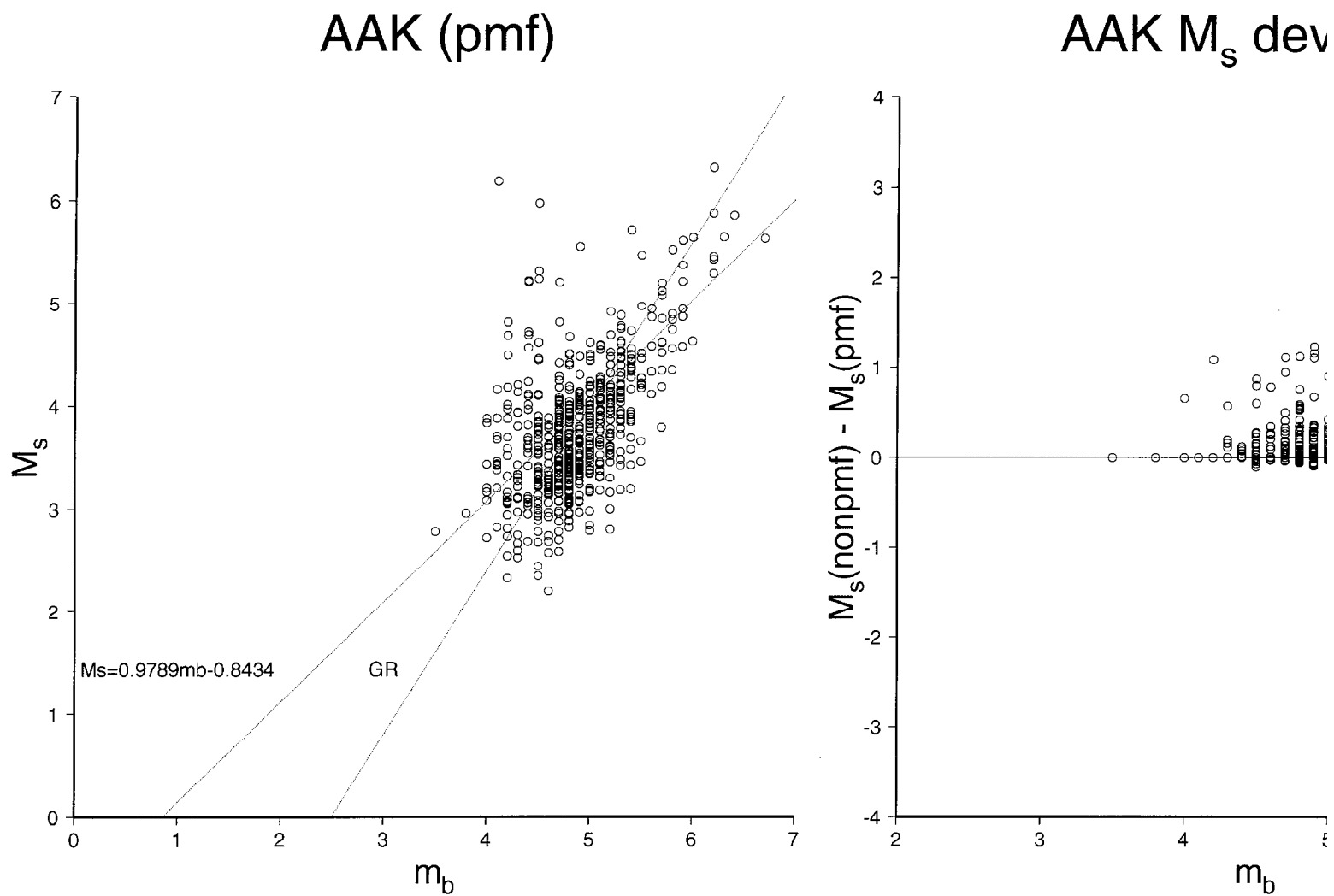
m_b

AAK M_s dev

$M_s(nonpmf) - M_s(pmf)$

m_b

Figure 5 - a) Surface wave magnitudes at station AAK calculated with a phase-matched filter and plotted as a function of body

difference between surface wave magnitudes calculated with and without use of the filter, also as a function of body wave mag
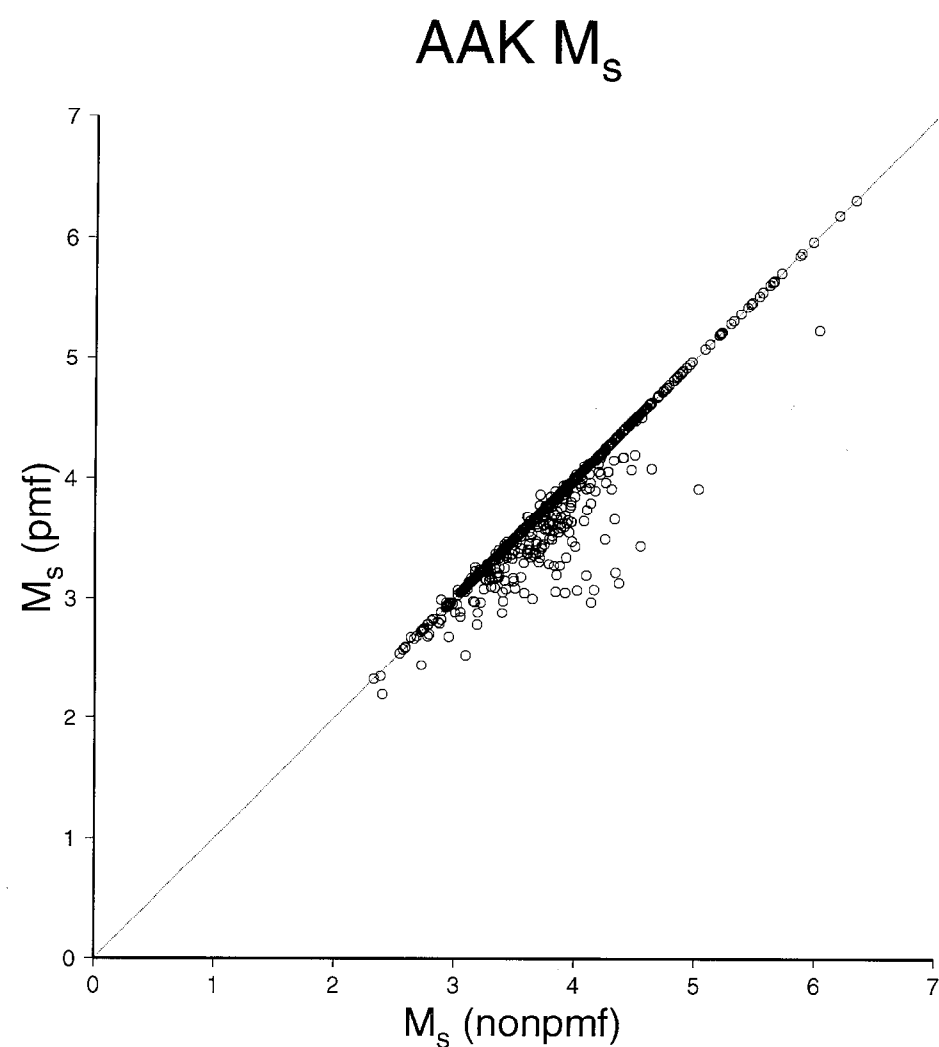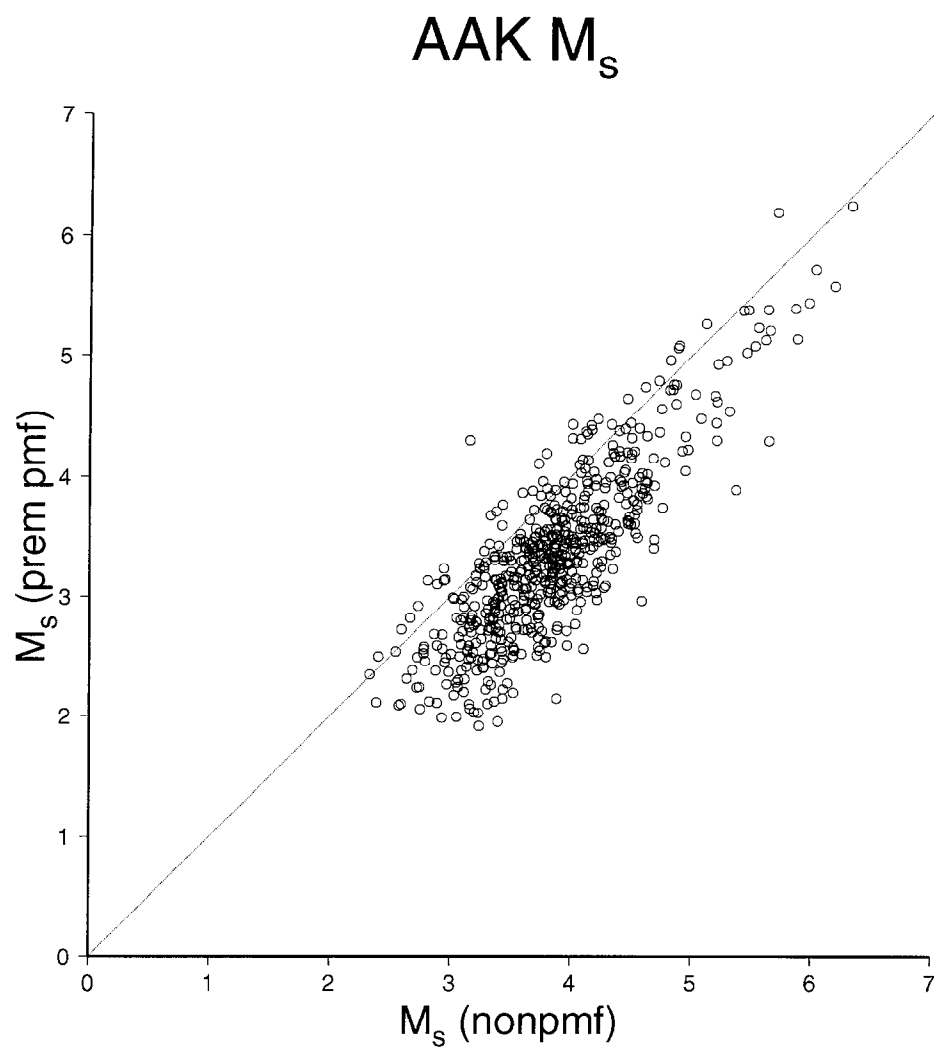
Figure 6. a) A comparison of surface wave magnitudes at station AAK calculated with and without a phase-matched filter constructed from group velocities predicted from the PREM model. b) The same comparison using phase-matched filters constructed from our surface wave tomography inversion results.